

SIMULATING THE DYNAMICS OF THE HUMBOLDT CURRENT SYSTEM
OFF PERU WITH A NONLINEAR TERRAIN-FOLLOWING
COORDINATE MODELMoacyr **ARAUJO**^{1,§},
Ralf **SCHWAMBORN**^{2,3, §}
Marcus A. **SILVA**¹¹Laboratório de Oceanografia Física Estuarina e Costeira,
Departamento de Oceanografia, Universidade Federal de
Pernambuco, 50740-550 Recife, Brazil.²Departamento de Zoologia, Universidade Federal de
Pernambuco, Recife, Brazil.³Present Address: Alfred Wegener Institute for Polar and
Marine Research, Dept. of Animal Ecology, D-27568
Bremerhaven, Germany.[§] CNPq fellows

Recebido em: 15/04/2006

Aceito em: 09/12/2006

RESUMO

As estruturas térmicas superficial e vertical, e a circulação oceânica do sudeste do Pacífico tropical (4°S-26°S / 70°W-91°W) são aqui analisadas. Trata-se da região onde parte da Sub-Corrente do Peru-Chile se desenvolve, influenciando sobre a distribuição dos componentes bióticos e abióticos ao longo da costa do Peru, e contribuindo para a variabilidade climática sobre o continente Sul Americano. O sistema de modelagem oceânica regional (ROMS) é então utilizado para simular o ciclo sazonal da circulação oceânica com o emprego de uma malha horizontal anisotrópica (1/2°-1/6°) e 20 camadas verticais ajustadas à topografia variável. Através desta resolução foi possível ilustrar a complexidade dos fenômenos de meso-escala que ocorrem na região. A estrutura térmica superficial simulada correspondeu às observações de satélite, e confirmaram a presença de águas oceânicas mais quentes (e mais salinas) adjacentes à costa do Peru em Janeiro, em comparação ao mês de Julho, quando águas mais frias (e menos salinas) são observadas. Os resultados numéricos também reproduziram satisfatoriamente a evolução espaço-temporal das correntes de fronteira leste, bem como os mecanismos de ressurgências nas regiões costeiras de Paita e Callao. Futuros esforços de modelagem matemática desta região serão direcionados à aplicação de malhas de alta resolução acopladas (1/12°, 1/16°), com a consideração de rotinas biogeoquímicas e ecológicas acopladas aos processos físicos.

Palavras-Chave: Pacífico tropical Leste, Temperatura de superfície, Dados de satélite, Ressurgência costeira, ROMS.

ABSTRACT

Surface and vertical thermal structures and ocean circulation are explored in the south-eastern tropical Pacific (4°S-26°S / 70°W-91°W). That region, where part of the Peru Chile Undercurrent (PCUC) flows is of prime interest for its influence over the distribution of biotic and abiotic compounds along the Peru edge, and by contributing to the climatic variability over South America. The Regional Ocean Model System (ROMS) is used here to simulate a seasonal cycle of the ocean circulation with an anisotropic horizontal grid (1/2°-1/6°) and 20 terrain-following layers. Such a high-resolved regional model can illustrate the complexity of the mesoscales phenomena which occur in that region. Simulated thermal structure at the upper ocean layers agrees rather well with satellite data set, and confirms that the waters off the Peruvian coast present warmer (and more saline) conditions in January, as compared to July, when colder (and lower salinity) waters prevail. Furthermore numerical results also reproduced the space-time evolution of the eastern boundary currents and the upwelling mechanisms in the areas off Paita and Callao with promising accuracy. Future efforts will concentrate on nesting of higher resolution grids (1/12°, 1/16°) and the linkage of biogeochemical and ecological routines with physical processes.

Keywords: Eastern tropical Pacific, Surface temperature, Satellite data, Coastal upwelling, ROMS.

INTRODUCTION

Eastern boundary current ecosystems (*e.g.* California, Canary, Humboldt and Benguela Current regions) support huge fish stocks, which provides about one third of the world's total catch of fish (MENDELSSOHN & SCHWING, 2002). Among these, the largest and most extensively studied upwelling area is the Humboldt Current System (HCS). There, upwelling cells and filaments are concentrated closely to the narrow continental shelf, where most of the biological production occurs (MARIN *et al.*, 2001; ESCRIBANO *et al.*, 2004). In the ENSO cycle, the warm phase (El Niño: EN) and cold phase (La Niña: LN) cause differences in the coastal upwelling in the Humboldt Current area and have both positive and negative socioeconomic, ecological and infrastructural implications in Peru and other countries. The aim of the CENSOR project is to enhance the detection, compilation and understanding of EN and LN effects on coastal marine environments and resources. One of the basic tools for the evaluation and prediction of ecosystem-scale consequences of climatic and oceanographic changes is the construction of appropriate models. For the upwelling areas off Peru, recent efforts have been invested in the construction of regional climate (GARREAUD & MUNOZ, 2004), sea level dynamics (CLARKE & AHMED, 1999), population (MAJLUF *et al.*, 2002), and trophic (JIANG & CHAI, 2005; MOLONEY *et al.*, 2005) models. First attempts to construct a two-dimensional simulation model of the physical-biological coupling were undertaken by Carr (2003). However, her model lacked any spatial resolution and relied on rough concepts of the main oceanographic

processes. For the construction of spatially discrete physical-biological models, first it is crucial to have reliable, high-resolution models of the current and water mass distributions on relevant scales.

In this paper, we use a 3-D regional ocean modeling approach for a simulation of the seasonal variability of the HCS off Peru, which will be the base of a future high-resolution physical-biological model. This is the contribution of the physical oceanography working group at UFPE to the multi-lateral research project CENSOR (www.censor.name). CENSOR (*Climate Variability and El Niño Southern Oscillation: Implications for natural coastal resources and management*) is a research and academic network dedicated to promote research initiatives, operational and monitoring activities, and training at several levels in the subjects of climate and climate variability, which aims to enhance the detection, compilation and understanding of El Niño and La Niña effects on coastal marine environments and resources. In the following sections, we describe the study area, the material and methods, the results and discussion. In the last section, conclusions of this work are presented.

STUDY AREA

The study area is comprised within 4°S and 26°S, and 70°W and 91°W (Figs. 1). The dominant water masses in the region are: Subtropical Surface Water (SSW), the Subantarctic Water (SAW), and Equatorial Subsurface Waters (ESSW).

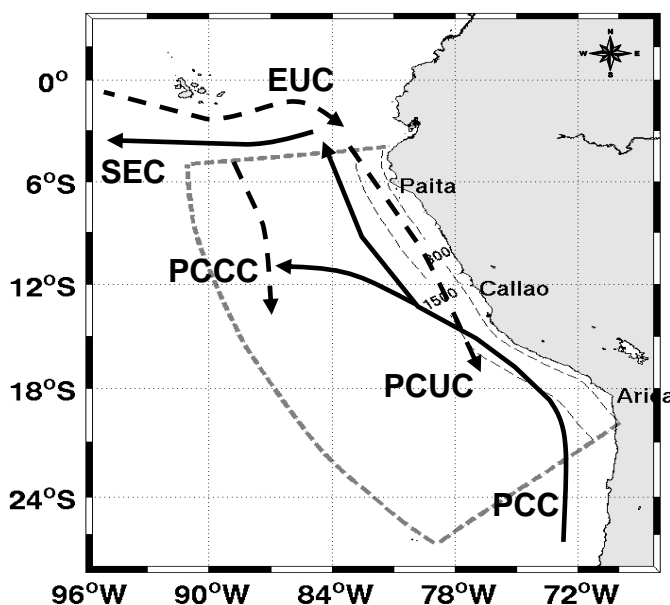


Figure 1 - Oceanic circulation scheme at the study area. Poleward under and counter currents are represented by dashed-bold lines, while equatorward

near-surface currents are in solid lines. The model integration domain and the near shore 200m and 1500m isobaths are also plotted.

SAW may occur interacting with SSW from surface to depth 40 m along coast in EN years. In the nearshore ESSW contribution may appear to the upper layer, depending on upwelling intensity. The ESSW is found between 100 and 300 m, normally (ESCRIBANO et al., 2004). However, Blanco et al. (2001) describe its presence at surface, noted by low-oxygen water, mainly during upwelling season (austral spring/summer), below our study area. According to Bakun & Nelson (1991), inside our study area, strong upwelling process occurs during austral winter. Strub et al. (1998) defines the SAW with cold temperatures (14°C) and less salinity (34.3-34.8), whereas SSW has temperatures greater than 18.5°C and salinity range between 34.9 and 35.7.

The current system of this area is composed by: the Peru Coastal Current (PCC), shallow and mostly in offshore areas. This flows equatorward with cold and salty water, associated with coastal upwelling; the Peru Chile Undercurrent (PCUC), which flows poleward over the slope; and by the Peru Chile Counter Current (PCCC) flowing poleward, mostly offshore. The PCC also known as the Humboldt Current feeds the South Equatorial Current (SEC) at 4°S . Its seasonal cycle is not well known, but measurements indicate a maximum velocity in winter (FIEDLER, 1994; PENVEN et al., 2005). The PCUC has a maximum core velocity of 15 cm.s^{-1} and depth between 100m and 150m depth near Callao (HUYER, 1980). Penven, et al. (2005) demonstrate that the depth of PCUC over Coriolis parameter is constant. Thus PCUC deepens as it flows away from the equator. Shaffer et al. (1999) observed at 30°S the core of the PCUC at 220 m, with mean flow of 12.8 cm.s^{-1} . The PCUC is originated in EUC southern branch, after EUC splits with Galapagos Island, near equator (LUKAS, 1986; PENVEN et al., 2005).

MATERIAL AND METHODS

ROMS is an ocean model previously adapted in different regions of the world ocean (HAIDVOGEL et al., 2000; MALANOTTE-RIZZOLI et al., 2000; SHE & KLINCK, 2000; PENVEN et al., 2000, 2001a,b; MCCREADY & GEYER, 2001; LUTJEHARMS et al., 2003). The model solves the free surface primitive equations in an Earth-centered rotating environment based on the classical Boussinesq approximation and hydrostatic vertical momentum balance. Coastline and solid bottom follow curvilinear coordinates, which allows minimizing the number of dead points in computing the solution. In this version of the run, surface wind stress forcing, open-ocean outgoing wave radiation, heat and water fluxes, coastal river inflows, bottom drag, and other components. Upstream advection is treated with a third-order scheme that enhances the solution through the generation of steep gradients as a function of a given grid size (SHCHEPETKIN & MCWILLIAMS, 1998). Unresolved vertical subgrid-scale processes are parameterized by an adaptation of the non-local K-profile planetary boundary layer scheme (LARGE et al., 1994). A complete description of the model may be found in Haidvogel et al. (2000), and Shchepetkin & McWilliams (2005).

The study case presented here concerns the ocean area off-Peru, where the Humboldt Current develops. Integration domains are comprised within 4°S and 26°S, and 70°W and 91°W (Fig. 2). An anisotropic curvilinear horizontal grid, with spatial resolution between $1/2^\circ$ and $1/6^\circ$, was used for simulations, resulting in 50 x 50 horizontal mesh cells. Vertical discretization considers 20 sigma-levels. Bottom topography was derived from a 2' resolution database ETOPO2 (SMITH & SANDWELL, 1997), and a "slope parameter" $r = \nabla h/h < 0.20$ has been used to prevent errors in the computation of pressure gradient (HAIDVOGEL et al., 2000). At the three open boundaries (north, east and south) an active, implicit, upstream biased radiation condition connects the model solution to the surrounding ocean (MARCHESIELLO et al., 2001, 2003). Horizontal Laplacian diffusivity inside the integration domain is zero, and a 4-point smooth increasing is imposed (up to $10^4 \text{ m}^2.\text{s}^{-1}$) in sponge layers near open ocean boundaries. The model equations are subjected to no-slip boundary conditions along the coastline.

A basin scale seasonal hydrology derived from World Ocean Atlas 2001 (WOA2001) database (monthly climatology at $1^\circ \times 1^\circ$ resolution) (LEVITUS, 1982; LEVITUS & BOYER, 1994) is used to infer thermodynamics (temperature and salinity) and geostrophy induced currents at the open boundaries. The oceanic circulation was forced at the sea surface by winds, heat fluxes and fresh water fluxes derived from the Comprehensive Ocean-Atmosphere Data Set (COADS) monthly fluxes data at $0.5^\circ \times 0.5^\circ$ resolution (DA SILVA et al., 1994).

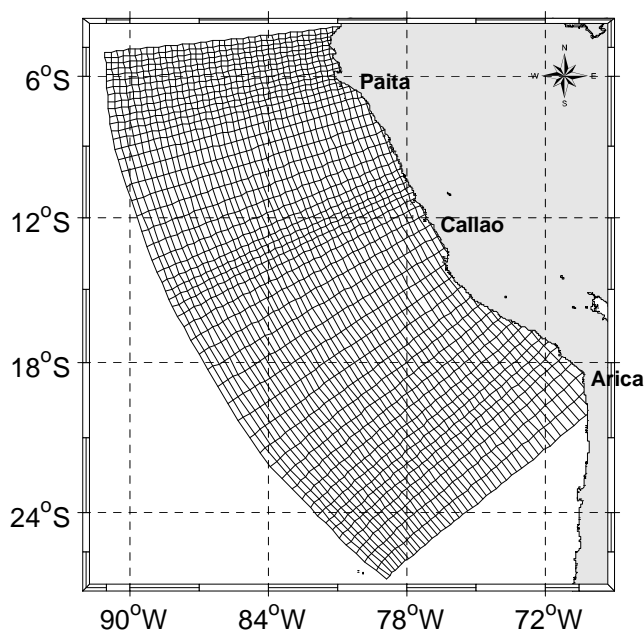


Figure 2 - Study area showing model integration domains with the horizontal grid lines.

The model runs from a state of rest (month of January) during 10 years. The steady state is statistically achieved after a spin-up period of about one year. All the numerical results examined here correspond to different averages of the last year of simulation.

At the three lateral open boundaries (North, East and South) an active, implicit, upstream biased, radiation condition connects the model solution to the ocean surroundings (MOORE et al., 2004). The model equations were subject to no-slip boundary conditions at solid boundaries. A basin scale seasonal hydrology derived from WOA2001 database (monthly climatology at 1° resolution) was used to infer thermodynamics (temperature and salinity) and geostrophy induced currents at the open boundaries.

RESULTS AND DISCUSSION

Model Spin-up

Using the forcings presented in previous sections, the model ran from a state of rest during 10 years. Figure 3 shows the time series of the integration domain kinetic energy (KE) from the model. It indicates that after a spin-up period of about one year, the model achieved a statistically steady state. All the numerical results examined correspond to the last year of simulation (year 10).

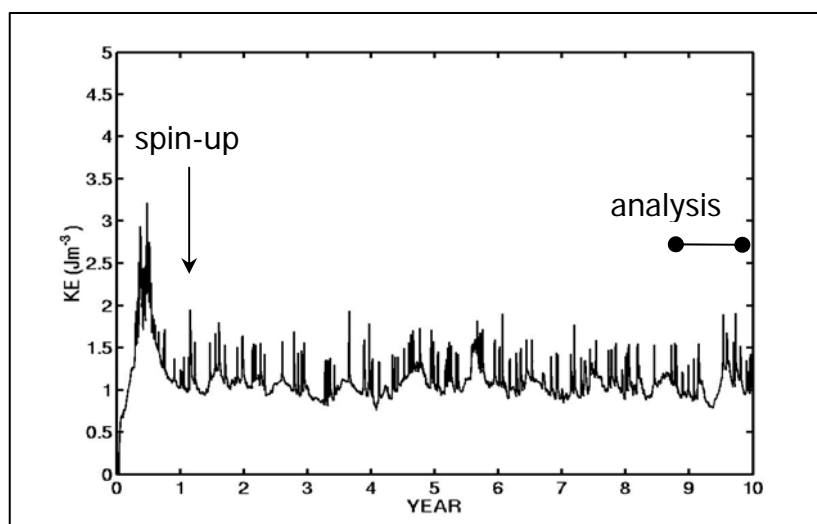


Figure 3 - Time series of integrated kinetic energy from the model during ten simulation years. All the numerical results examined correspond to the last year of simulation (year 10).

Sea Surface Temperature (SST)

As first illustrations of the model simulation, we present the month-averaged sea surface temperature (SST) patterns for January and July, *i.e.*

during two extreme seasonal conditions. These figures show mainly a seasonal meridional change in SST along the South Pacific eastern boundary. Offshore of the PCC and the PCUC (see Fig. 1), a tongue of warm water signifies the surface of the Peru-Chile Counter-Current (PCCC). The so-called South Pacific Warm Tongue (SPWT), marked by high values of SST ($> 22^{\circ}\text{C}$), extends off the coastline from the equator to about 12°S during austral winter (e.g. July, Fig. 4b). Six months later, during austral summer (e.g. January, Fig. 4a), these high SST values invade the whole studied zone, and warmer waters reach the 15°S . In liaison with that seasonal meridional extension, the SPWT pattern records seasonal zonal changes, with a more alongshore location during the summer. The seasonal extension of the cold waters ($< 18^{\circ}\text{C}$) near the coast also follows the meridional progression as that of the SPWT. Maxima of equatorward, upwelling favorable winds over the slope shift southward from the austral winter off Peru.

As also illustrated by these figures it is noted that the ROMS succeeds in resolving meso-scale dynamic processes. These phenomenas, which are particularly visible at the frontier between warm and cold waters on the ROMS results (Figs. 4a,b) when using a curvilinear horizontal grid resolution ($1/2^{\circ}$ - $1/6^{\circ}$), also appear with a slightly weaker accuracy on two examples of month-averaged observed SST by satellite using $1/12^{\circ}$ ($\cong 9,25$ km) resolution: one in January/2006 (Fig. 5a), the other one in July/2006 (Fig. 5b).

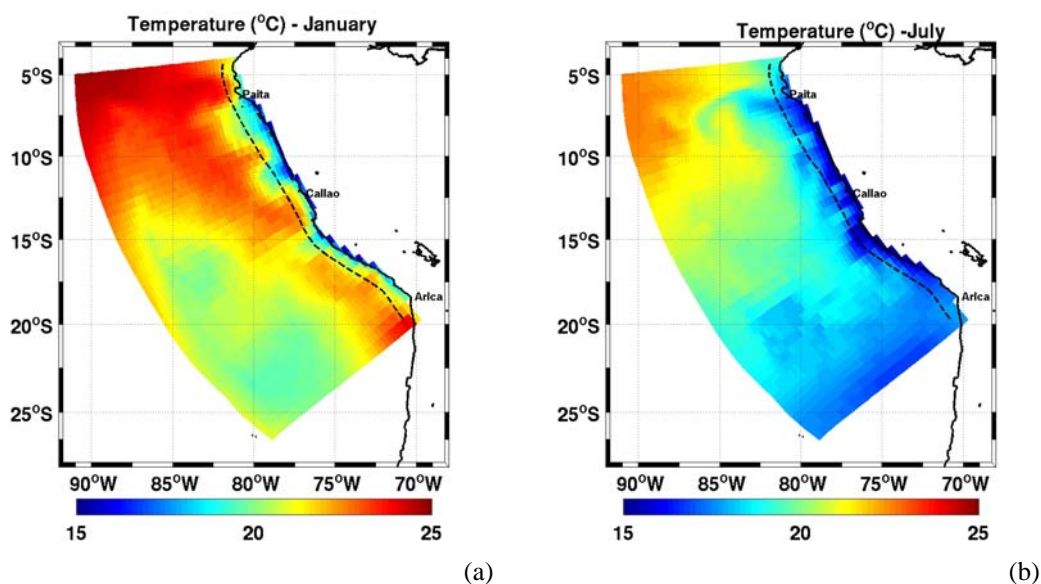


Figure 4 - Month-averaged Sea Surface Temperature (SST, $^{\circ}\text{C}$) obtained from ROMS simulations for: (a) January; and (b) July.

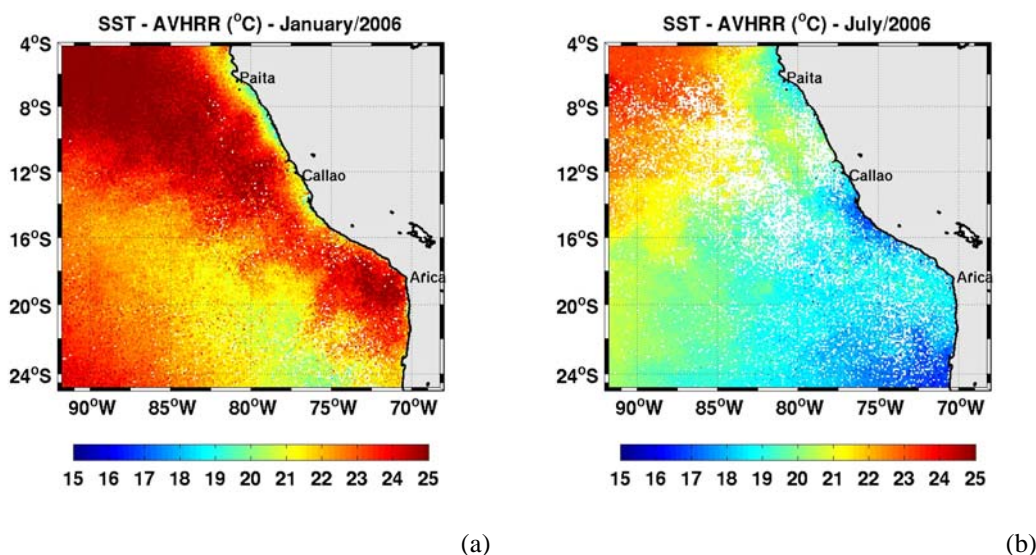


Figure 5 - Month-averaged Sea Surface Temperature (SST, °C) obtained from AVHRR satellite for: (a) January/2006; and (b) July/2006. White areas in figures are due to the absence of backscatter signals (cloudy areas).

Satellite data and numerical simulation results confirm that the waters off the Peruvian coast present warmer (and more saline, not shown here) conditions in January, as compared to July, when colder (and lower salinity) waters prevail. Horizontal distributions temperature and salinity issued from simulations indicate that SSW dominates at offshore surface waters in January, whereas SAW and ESSW are found nearshore.

Ocean Circulation and Coastal Upwelling

The seasonal changes in surface circulation in the study area are also indicated in Fig. 6. These results correspond to current vectors issued from model simulations for January and July scenarios. The general circulations during these months are responses to the combined effects of wind shear and Ekman pumping. Two convergence/off-shoreward zones may be identified from vector distributions in Fig. 8. These correspond to Paita Bay (5° S) and Callao site (12° S), where strong upwelling mechanisms take place.

Horizontal velocity vector ($|v|$, cm.s^{-1}) obtained from the model simulations kept in the range $0.3 \text{ cm.s}^{-1} \leq |v| \leq 34.3 \text{ cm.s}^{-1}$ (January) and $0.1 \text{ cm.s}^{-1} \leq |v| \leq 22.4 \text{ cm.s}^{-1}$ (July).

Sea measurements obtained by Brink et al. (1983) have indicated that below a thin surface Ekman layer, poleward flows dominate the subsurface and the shelf. Model results (see Fig. 7) demonstrate that at 50 m depth, the PCUC is already noticeable at the shore with speeds of about 8 cm.s^{-1} to 18 cm.s^{-1} . Part of this flow is fed by the EUC and the SECC that enters the model domain

at about 4°S . According to simulations, the SECC also feeds the PCCC that flows southward at about 7 cm.s^{-1} from a latitude of 6°S .

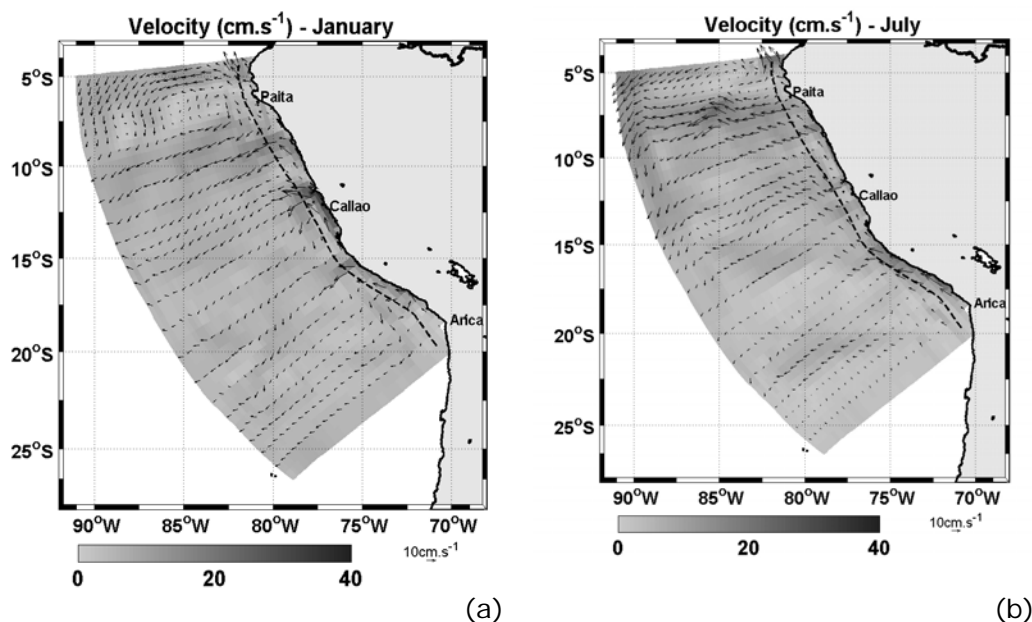


Figure 6 - Snap-shot of the surface horizontal velocity vector ($|v|$, cm.s^{-1}) obtained from ROMS for: (a) Mid-January; and (b) Mid-July.

The PCCC is shifting westward to leave the study area between 14°S and 18°S . This offshore veering could be a plausible explanation for the termination of the PCCC, as also proposed in the numerical studies of Peven et al. (2005).

Mean (month-averaged) meridional currents obtained from the ROMS simulation along zonal section 12°S (0-300m depth) are presented in Fig. 7 for January and July. Three density levels are indicated on the plots. The $\sigma_t = 24.5\text{ kg.m}^{-3}$ separates the upper Subtropical Surface Water (SSW) from the upper thermocline waters, near 40m. These waters occur offshore. The $\sigma_t = 26.8\text{ kg.m}^{-3}$ is the lower level of the water supplied by SAW mixed with ESSW, reaching the surface closer the coast.

The zonal sections show a clear representation of the Peru Coastal Current (PCC), a shallow and mostly in offshore areas that flows equatorward with cold and salty water associated with coastal upwelling; the Peru Chile Undercurrent (PCUC) flowing poleward over the slope, and the Peru Chile Counter Current (PCCC) flowing poleward and with its core placed offshore. Model results show the PCC-PCUC system skirting the coastline from surface to 500m, with a northward PCC transport with velocities from 2 cm.s^{-1} (July) to 16 cm.s^{-1} (January). In Fig. 7a the PCCC is flowing poleward with intensities of 4 cm.s^{-1} at 25m depth. All these results agree with previous numerical studies and experimental dataset (BRINK et al., 1983; HUYER et al., 1991; PENVEN et al 2005), confirming the skill of the regional modeling approach to reproduce the PCC-PCUC-PCCC dynamics.

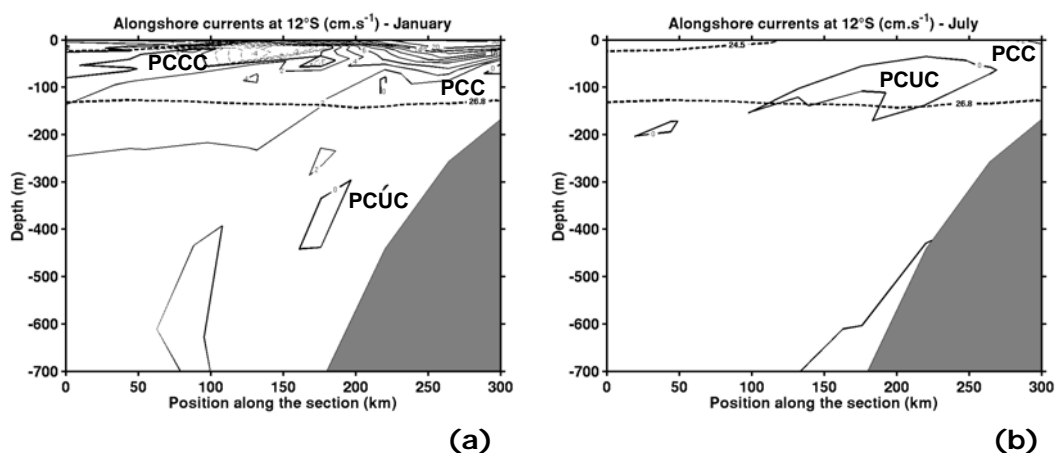


Figure 7 - Mass transport (month-averaged) across zonal sections at T12, 12°S for: (a) January; and (b) July. Positive (negative) values indicated by solid (dashed) lines for the zonal sections correspond to northward (southward) currents. Bold dashed lines indicate the rough boundaries between different water masses (see the text for details).

Wind data from COADS Climatology - 1854 to 1993 (DASILVA et al., 1994) indicate the predominance of the south/southwest winds, suggesting that favorable conditions for upwelling prevails year round. Strongest winds are present in the area during late spring and austral winter conditions, decreasing by late summer or fall. Bakun & Nelson (1991), achieve maximum cyclonic wind stress curl in austral winter along Peruvian shelf, but not off northern and central Chile, where maximum curl occurs in austral summer.

Mid-month snap-shots of the near shore vertical distributions of temperature (°C) at the transect T12 are presented in Fig. 8. This transect is situated along 12°S, at Callao site. The dashed ellipses in Fig. 8 show isothermal upwelling pointed out by simulations. These results correspond to thermal distributions issued from model simulations for January and July scenarios. Figure 8b confirms that stronger upwelling processes take place in July (austral winter), when isotherms are shifted up near the Peruvian coast.

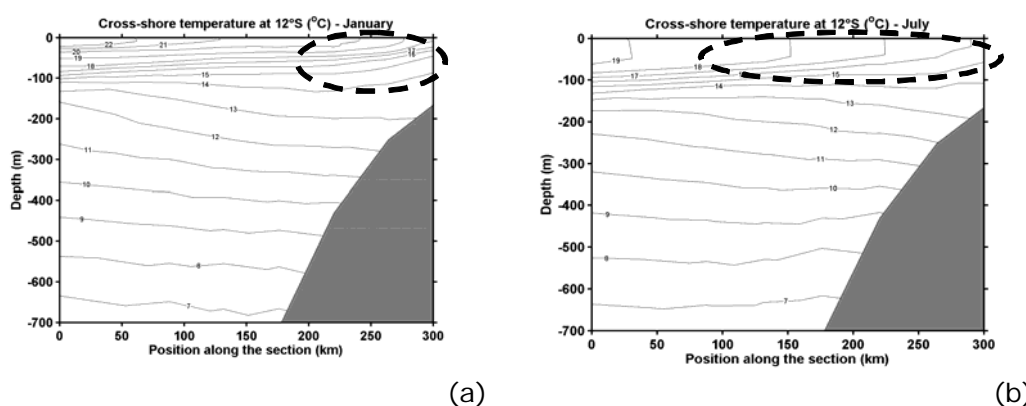


Figure 8 - Mid-month snap-shots of the vertical temperature distribution ($^{\circ}\text{C}$) near shore along transect T12. The dashed ellipses show isothermal shifting pointed out in simulations.

CONCLUSION

In this study we used a regional ocean model approach for investigating the thermohaline and circulation structures in the eastern Pacific boundary off-Peru. The first outputs of the ROMS confirm the extreme complexity of the oceanic circulation in this area. That is obviously the case along the eastern edge of the continent where many alongshore currents coexist and can interact. Numerical results allowed the identification of the most important dynamical features in the area. For example, the space-time evolutions (latitude x seasons) of the Sea Surface Temperature obtained in climatological simulations agrees well with the large and meso-scales standards observed from satellite data. By the same time, the seasonal variability of the upwelling mechanism are well reproduced along the Peru shore, when model results confirm stronger vertical displacements of subsurface waters during austral winter (July).

This primary study is very encouraging and the verified model adjustment to remote sensing and previous literature data seems to be promising. Three forthcoming approaches are as follows: (i) to use the ROMS forced by interannual boundary conditions with more refined grids ($1/12^{\circ}$, $1/16^{\circ}$), in order to investigate the intra-seasonal variability in this region; (ii) to perform various numerical experiments testing in more details the dynamics of the region, what could be, for instance, an useful tool to estimate the dispersion of the fish larvae in the Peru Chile Undercurrent (PCUC); and (iii) to improve the linking between biogeochemical/ecological routines and physical circulation part, especially for investigating nearshore transfer of plankton biomass and nutrients. In this case, the use of nested high-resolution grids for the coastal area will be a very useful technique. These studies are underway.

ACKNOWLEDGEMENTS

This study is part of the CENSOR project (www.censor.name), which is being financed in the context of the 6th framework as Specific Targeted Project INCO-CT2004-511071 by the European Commission. M. Silva wishes to thank CAPES/BRAZIL (Coordination for the Improvement of Higher Education Staff) for the scholarship support.

REFERENCES

- BAKUN, A.; NELSON, C. S., 1991. The seasonal cycle of wind-stress curl in subtropical eastern boundary current regions. **Journal of Physical Oceanography**, 21, 1815–1834.
- BLANCO, J.L.; THOMAS, A.C.; CARR, M.E.; STRUB, P.T., 2001. Seasonal climatology of hydrographic conditions in the upwelling region off northern

Chile. **Journal of Geophysical Research**, 106:11,451-11,467.

BRINK, K. H.; HALPERN, D.; HUYER, A.; SMITH, R. L., 1983. The physical environment of the Peruvian upwelling system. **Progress in Oceanography**, 12:185-305.

CARR, M.E., 2003. Simulation of carbon pathways in the planktonic ecosystem off Peru during the 1997-1998 El Nino and La Nina. **Journal of Geophysical Research**, Art. No. 3380 Dec 16 2003.

DA SILVA, A. M.; YOUNG, C. C.; LEVITUS, S., 1994. Atlas of surface marine data 1994, Vol. 1, algorithms and procedures, **NOAA Atlas NESDIS 6**. U.S. Department of Commerce, NOAA, NESDIS, USA, 74pp.

ESCRIBANO, R.; ROSALES, S. A.; BLANCO, J. L., 2004. Understanding upwelling circulation off Antofagasta (northern Chile): A three-dimensional numerical-modelling approach. **Journal of Coastal Research**, 24: 37-53.

FIEDLER, P. C., 1994. Seasonal and interannual variability of coastal zone color scanner phytoplankton pigments and winds in the eastern Pacific. **Journal of Geophysical Research**, 99:18,371–18,384.

GARREAUD R.D.; MUNOZ, R., 2004. The diurnal cycle in circulation and cloudiness over the subtropical southeast Pacific: A modeling study. **Journal of Climate** 17 (8): 1699-1710.

HAIDVOGEL, D. B.; ARANGO, H. G.; HEDSTROM, K.; BECKMANN, A.; MALANOTTE-RIZZOLI P.; SHCHEPETEKIN, A. F., 2000. Model evaluation experiments in the North Atlantic basin: simulations in nonlinear terrain-following coordinates. **Dynamics of Atmosphere and Oceans**, 32: 239-281.

HUYER, A., 1980. The offshore structure and subsurface expression of sea level variations off Peru, 1976 – 1977. **Journal of Physical Oceanography**, 10:1755–1768.

HUYER, A.; KNOLL, M.; PALUZKIEWICZ, T.; SMITH, R. L., 1991. The Peru Undercurrent: A study in variability. **Deep Sea Research**, 39:247–279.

JIANG, M.; CHAI, F., 2005. Physical and biological controls on the latitudinal asymmetry of surface nutrients and pCO₂ in the central and eastern equatorial Pacific **Journal of Geophysical Research**, 110, C6.

LARGE, W. G.; MCWILLIAMS, J. C.; DONEY, S. C., 1994. Oceanic vertical mixing: a review and a model with a nonlocal boundary layer parametrization. **Reviews in Geophysics**, 32, 363-403.

LEVITUS, S., 1982. Climatological Atlas of the World Ocean. **U. S. Gov. Printing Office**, Washington D.C., USA, 173 p.

LEVITUS, S.; BOYER, T., 1994. World Ocean Atlas 1994. Vol. 3 and 4. **NOAA Atlas NESDID 16**, U. S. Gov. Printing Office, Washington D.C., USA.

LUTJEHARMS, J. R. E.; PENVEN, P.; ROY, C., 2003. Modelling the shear edge

eddies of the southern Agulhas Current. **Continental Shelf Research**, 23, 1099-1115.

LUKAS, R., 1986. The termination of the equatorial undercurrent in the eastern Pacific. **Progress in Oceanography**, 16: 63– 90.

MCCREADY, P.; GEYER, G. R., 2001. Estuarine salt flux through an isohaline surface. **Journal of Geophysical Research**, 106, 11629-11637.

MAJLUF P.; BABCOCK, E. A.; RIVEROS, J.C.; SCHREIBER, M.A.; ALDERETE, W., 2002. Catch and bycatch of sea birds and marine mammals in the small-scale fishery of Punta San Juan, **Peru Conserv. Biol.** 16 (5): 1333-1343.

MARIN, V.; ESCRIBANO, R.; DELGADO, L. E.; OLIVARES, G.; HIDALGO, G., 2001. Nearshore circulation in a coastal upwelling site of northern Humboldt Current System. **Journal of Coastal Research**, 21: 1317-1329.

MENDELSSOHN, R.; SCHWING, F. B., 2002. Common and uncommon trends in SST and wind stress in the California and Peru-Chile current systems. **Progress in Oceanography**, 105: 141-162.

MALANOTTE-RIZZOLI, P.; HEDSTRÖM, K.; ARANGO, H. G.; HAIDVOGEL, D. B., 2000. Water mass pathways between the subtropical and tropical ocean in a climatological simulation of the North Atlantic. **Dynamics of Atmosphere and Oceans**, 32, 331-371.

MARCHESIELLO, P.; MCWILLIAMS, J. C.; SHCHEPETIN, A. F., 2001. Open boundary conditions for long-term integration of regional oceanic models. **Ocean Modelling**, 3, 1-20.

MARCHESIELLO, P.; MCWILLIAMS, J. C.; SHCHEPTKIN, A. F., 2003. Equilibrium structure and dynamics of the California Current System. **Journal of Physical Oceanography**, 33, 753-783.

MENDELSSON, R.; SCHWING, F.B., 2002. Common and uncommon trends in SST and wind stress in the California and Peru-Chile current systems. **Progress in Oceanography**, 53: 141-162.

MOLONEY C.L.; JARRE, A.; ARANCIBIA, H.; BOZEC, Y.M.; NEIRA, S.; ROUX, J.P.; SHANNON, L.J., 2005. Comparing the Benguela and Humboldt marine upwelling ecosystems with indicators derived from inter-calibrated models. **ICES Journal of Marine Science**, 62 (3): 493-502.

MOORE, A. M.; ARANGO, H. G.; DI LORENZO, E.; CORNUELLE, B. D.; MILLER, A. J.; NEILSON, D. J., 2004. A comprehensive ocean prediction and analysis system based on the tangent linear and adjoint of a regional ocean model. **Ocean Modelling**, 7, 227-258.

PENVEN, P.; ROY, C.; COLIN DE VERDIÈRE, A.; LARGIER, J., 2000. Simulation and quantification of a coastal jet retention process using a barotropic model. **Oceanological Acta**, 23, 615-634.

PENVEN, P.; ROY, C.; LUTJEHARMS, J. R. E.; COLIN DE VERDIÈRE, A.; JOHNSON, A.; SHILLINGTON, F.; FRÉON, P.; BRUNDRIT, G., 2001a. A regional hydrodynamic model of the Southern Benguala. **South African Journal of Science**, 97, 472-476.

PENVEN, P.; LUTJEHARMS, J. R. E.; MARCHESIELLO, P.; ROY, C.; WEEKS, S. J., 2001b. Generation of cyclonic eddies by the Agulhas Current in the lee of the Agulhas Bank. **Geophysical Research Letters**, 27, 1055-1058.

PENVEN, P.; ECHEVIN, V.; PASAPERA, J.; TAM, J., 2005. Average circulation, seasonal cycle, and mesoscale dynamics of the Peru Current System: A modeling approach. **Journal of Geophysical Research**, 10:doi:10.1029/2005JC002945.

SHCHEPETKIN, A. F.; MCWILLIAMS, J. C., 1998. Quasi-monotone advection schemes based on explicit locally adaptive dissipation. **Monthly Weather Review**, 126, 1541-1580.

SHCHEPETKIN, A. F.; MCWILLIAMS, J. C., 2005. The Regional Oceanic Modeling System (ROMS): a split-explicit, free surface, topography-following-coordinate oceanic model. **Ocean Modelling**, 9: 347-404.

SMITH, W. H. F.; SANDWELL, D. T., 1997. Global seafloor topography from satellite altimetry and ship depth soundings. **Science**, 277: 1957-1962.

SHAFFER, G.; HORMAZABAL, S.; PIZARRO, O.; SALINAS, S., 1999. Seasonal and interannual variability of currents and temperature off central Chile. **Journal of Geophysical Research**, 104: 29,951-29,961

SHE, J.; KLINCK, J. M., 2000. Flow near submarine canyons driven by constant wind. **Journal of Geophysical Research**, 105, 28671-28694.

STRUB, P. T.; MESIAS, J. M.; MONTECINO, V.; RUTLLANT, J.; SALINAS, S., 1998. **Coastal ocean circulation off western South America**. In: A. R. Robinson ; K. H. Brink (eds.) , The Sea, vol. 11, pp. 273– 314, John Wiley.